Vol. 20, No. 2 (2021) 941-954
Revista Mexicana de Ingeniería Química

Removal of methylene blue dye using *Nostoc commune* biomass: kinetic, equilibrium and thermodynamic study

Remoción del colorante azul de metileno mediante biomasa del *Nostoc commune*: estudio cinético, equilibrio y termodinámico

C. Lavado-Meza[1]*, Y. J. O. Asencios[2], G. Cisneros-Santos[3], I. Unchupaico-Payano[4]

[1]*Faculty of environmental engineering, Continental University (UC), Huancayo, Peru.*
[2]*Institute of Marine Science, Federal University of São Paulo (UNIFESP), Santos-SP. Brazil.*
[3]*Professional School of International Business Administration Intercultural University of the Central Jungle Juan Santos Atahualpa (UNISCJSA), Chanchamayo, Peru.*
[4]*Faculty of Zootechnics, National University of Central Peru (UNCP), Huancayo, Peru.*

Received: January 2, 2021; Accepted: March 12, 2021

Abstract

In the present work, the elimination of the cationic Methylene Blue (MB) dye is reported using the dry powder of *Nostoc commune* (NC). The results of the Fourier Transform Infrared Spectroscopy (FTIR) analysis corroborated the presence of functional groups such as hydroxyls, carbonyls, and amines. The scanning analysis microscopy shows the change in morphology after the biosorption of MB. In a stationary (batch) system, the experimental parameters that affect biosorption, such as NC dose, pH, temperature, and initial MB concentration were evaluated. The experimental data of the isotherm fit better to the Langmuir model. The maximum biosorption capacity of MB of 158.7 mg/g was obtained with a dose of 1 g NC/L, pH 8, and contact time of 120 min. The kinetic data were better adjusted to the pseudo-second-order model, which indicates that biosorption seems to be controlled by chemisorption, the intraparticle diffusion model indicates that diffusion in the pores is the limiting factor throughout the biosorption process. The thermodynamic parameters indicated that at all the temperatures evaluated (293, 303, and 313 K) the biosorption of MB on NC was a spontaneous, favorable, and exothermic process. The results showed that NC can be used to remove cationic dyes from wastewater.

Keywords: Biosorption, water treatment, cyanobacteria, cationic dye.

Resumen

En el presente trabajo de investigación informamos la capacidad de eliminación del colorante catiónico azul de metileno (AM) usando el polvo seco del *Nostoc commune* (NC). Los resultados del FTIR corroboraron la presencia de grupos funcionales como hidroxilos, carbonilos y aminas los cuales estarían asociados a la remoción del AM. El análisis de microscopía electrónica de barrido muestra un cambio en la morfología del biosorbente NC antes y después de la biosorción. En un sistema discontinuo, se evaluaron los parámetros experimentales que afectan el proceso de biosorción, como la dosis de NC, el pH, temperatura y concentración inicial de AM. Los datos experimentales de la isoterma se ajustaron mejor al modelo de Langmuir. Se obtuvo la capacidad máxima de biosorción del AM de 158.7 mg/g con una dosis de 1 g NC/L, pH 8 y tiempo de contacto de 120 min. Los datos cinéticos se ajustaron mejor al modelo de pseudo-segundo orden lo que indica que la biosorción parece estar controlada por la quimisorción, el modelo de difusión intraparticular indica que la difusión en los poros es el factor limitante durante todo el proceso de biosorción. Los parámetros termodinámicos indicaron que la biosorción del AM sobre NC fue un proceso espontáneo, favorable y exotérmico. Los resultados mostraron que el NC puede ser usado para remover colorantes catiónicos de aguas residuales.

Palabras clave: Biosorción, tratamiento de aguas, cianobacteria, colorante catiónico.

1 Introduction

Water pollution is one of the main concerns in recent decades due to accelerated industrialization and urbanization (Shooto *et al*., 2020). Synthetic dyes are widely used in the textile, paper, food, cosmetic and pharmaceutical industries (Alver *et al*., 2020). The presence of synthetic dyes in water prevents the penetration of light, delaying photosynthesis and reducing the re-oxygenation of the water (Wahlström *et al*., 2020).

* *Corresponding author. E-mail*: clavado@uniscjsa.edu.pe
https://doi.org/10.24275/rmiq/IA2291
ISSN:1665-2738, *issn-e*: 2395-8472

Due to the presence of complex aromatic molecules in their structures, they are resistant to photodegradation, biodegradation, and oxidation, which are relatively difficult to treat and persist in the environment (Daneshvar *et al*., 2017). Most synthetic dyes are toxic and carcinogenic; therefore, they could be responsible for serious environmental damage and also pose a threat to public health (Han *et al*., 2020). Methylene blue (MB) whose molecular formula is C16H18ClN3S is a cationic synthetic dye that is widely used in medical staining agents, diagnostic tests, and fiber dyes in the textile industries. The high dose of MB causes serious skin problems, eye irritation, vomiting, methemoglobinemia, profuse sweating, mental confusion, respiratory toxicity, etc.(Akbari *et al*., 2015; Yagub *et al*., 2014). Several physical, chemical, and biological techniques have been developed to remove synthetic colorants. Biosorption is a technique that has been used for the decolorization of wastewater where a solid adsorbent is used to attract the dye molecule and finally lead to its elimination from the aqueous medium. For this purpose, abundant and low-cost waste materials are used, such as plant materials, industrial and agricultural waste (Fomina & Gadd, 2014), non-living microbial agents such as bacteria, fungi, yeasts, algae, and cyanobacteria (Gupta & Rastogi, 2008). According to Tatjana *et al*. (2018), the functional groups of proteins and exopolysaccharides present in cyanobacteria play a very important role in the mechanism of the biosorption of organic and inorganic contaminants. In the removal of the methylene blue dye, various bioabsorbents have been used such as mucuna beans (Shooto *et al*., 2020), *Ulva fasciata* and *Sargassum dentifolium* (Moghazy *et al*., 2019), *Chlorella pyrenoidosa* and *Spirulina* (Lebron *et al*., 2018) determining the effect of parameters such as pH, adsorbent dose, contact time, temperature and initial concentration, in the removal of methylene blue.

There are studies on the use of Nostoc biomass for the removal of some heavy metals such as Pb, Zn, Cd, and Cr (Diengdoh & Syiem, 2017; Gupta & Rastogi, 2008; Morsy *et al*., 2011), but there is little information of its use in the treatment of synthetic colorantsIs important and advantageous to carry out biosorption studies with *Nostoc commune* (NC) since it grows in extreme conditions and low in nutrients, it does not produce toxic substances compared to other bacteria and fungi, besides, it is capable of photosynthesis (Patel et al., 2019). These characteristics mean that the *Nostoc commune* could be grown outdoors or in laboratory cultures on a large scale and at low cost, therefore, providing a cheap, reliable, and constant supply of biomass for eventual expansion works, in this way to be used sustainably.

The objective of the present study was to evaluate the biosorption capacity of MB using the dry powder of *Nostoc commune* as a biosorbent. For which the influence of pH, initial MB concentration, contact time, and temperature on the MB biosorption capacity was evaluated. The experimental data was evaluated using kinetic, isothermal, and thermodynamic models to try to explain the biosorption mechanism of MB on NC.

2 Materials and methods

2.1 *Nostoc commune biosorbent*

The biomass used in this study was prepared from the *Nostoc commune*, these gelatinous colonies were collected in the town of Pampa Cruz in the Junín Region, in Peru. The straw and soil residues were removed with abundant distilled water, subsequently, they were dried in the oven at 60ºC for 3 days, the dry material was ground and sieved to a 70 μm mesh, thus obtaining the dry powder of the NC.

2.2 *Biosorbent characterization*

The functional groups present on the biosorbent surface were identified by Fourier Transform Infrared Spectroscopy (FTIR) in a SHIMADZU FTIR-8700 Spectrophotometer, the sample was analyzed in a spectral range of 4000 to 400 cm^{-1}. The determination of the acid groups was carried out following the Boehm method, described by Aygun, *et al*. (2003) in which a strong base, such as NaOH, is used to neutralize the acid centers present on the surface of the NC. Scanning Electron Microscopy (SEM) Model SU 8230 Evo15, Hitachi Brand was used to study the morphology of the adsorbent surface. To determine the point zero charge (p_{HPZC}), we proceeded according to what was reported by Moghazy *et al*. (2019) for this, 0.05 g of biomass was mixed with 50 mL of an aqueous solution with different initial pH values (pH_o) ranging from 1 to 12 and the final pH (pH_f) was determined after 24 h of equilibrium. To vary the pH of the solutions, 1 M HCl and NaOH solutions were used. The values of ΔpH ($\Delta pH = pH_o - pH_f$) versus initial pH (pH_o) were plotted, the p_{HPZC} was obtained from the graph when $\Delta pH = 0$.

2.3 Biosorbent studies

A stock solution of MB (Reag. Ph Eur) of 500 mg/L was prepared from it, the different necessary concentrations were prepared, the biosorption of MB was carried out in a discontinuous system composed of multiple shaking equipment and Erlemenyer flasks in which the AM solutions and the NC biomass were put in contact at a speed 150 RPM, room temperature (20oC) using different doses of NC (0.025 - 6 g/L). To determine kinetic equilibrium, the experiments were carried out at different time intervals (5-180 min) (Tejada-Tovar *et al*., 2020). The biosorption balance was evaluated at different initial concentrations of MB (20 - 400 mg/L of MB). The study of the influence of pH was carried out adjusting the pH to values between 1.0 - 8.0 with HCl and NaOH solutions. The study of the influence of temperature was carried out with three different temperatures (293, 303, and 313 K) with a fixed dose of NC of 1g/L and two different initial concentrations of MB of 100 and 200 mg/L. In each case, after the experiments, the phases were separated by filtration and the MB concentrations in the samples were measured through a UV-Vis spectrophotometer (Beckman Du 64 UV/VIS) at a wavelength of 663 nm. All experiments were carried out in triplicate and the results presented are the corresponding average and the respective standard deviations.

2.4 Desorption studies

For the desorption study, 0.1 g of NC was put in contact with 50 mL of MB with a concentration of 100 mg/L (under continuous stirring), it was kept stirring for 2 h. The unadsorbed dye solution was then separated by filtration. The spent biosorbent was dried at 333 K for 24 h. This material was mixed and stirred (150 RPM) with 50 mL of HCl at different concentrations (0.1, 0.5, and 1 M) (Eren *et al*., 2020). The adsorbed and desorbed MB concentration was examined with a UV-vis spectrophotometer.

2.5 Data analysis

The amount of MB retained by the biosorbent (q_e) in mg/L and the % Removal were calculated using equations 1 and 2 respectively.

$$q_e = \frac{(C_o - C_e) \times V}{M} \tag{1}$$

$$\%R = \frac{(C_o - C_e)}{C_o} \tag{2}$$

where: C_o and C_e are the initial and final concentration of MB in the solution (mg/L) before and after biosorption respectively, M is the mass of NC (g), and V the volume of the solution (L) (Salazar-Pinto *et al*., 2021).

The biosorption kinetic data obtained were adjusted to the kinetic models described in Table 1.

The experimental data at equilibrium were evaluated using the Langmuir and Freundlich isotherm models, whose linearized forms are expressed in the Table 2.

Table 1. Kinetic adsorption models.

Model	**Equation**	**Parameters**
Largergren or Pseudo-first order	$\log(q_e - q_t) = \log(q_e) - \frac{k_1}{2.303} t$	q_e (mg/g): adsorption capacity qt (mg/g): the amount of MB retained per unit mass of biosorbent in time t
Pseudo-Second order	$\frac{t}{q_t} = \frac{1}{k_2 q_e^2} + \frac{t}{q_e}$ $h = k_2 q_e^2$	k_1 (1/min): the first-order kinetic constant k_2 (g/mg min): rate constant adsorption h (mg/g min): initial adsorption rate
Intraparticle diffusion	$q_t = k_{id} t^{1/2} + B$	K_{id} (mg/g $\text{min}^{1/2}$): intraparticle diffusion rate constant B (mg/g): constant related to the thickness of the adsorbent boundary layer

Source: (Shooto *et al*., 2020).

Table 1. Kinetic adsorption models.

Model	Equation	Parameters
Langmuir	$\frac{C_e}{q_e} = \frac{1}{q_{max}b}$ ‘ $+ \frac{C_e}{q_{max}}$	q_e (mg/g): adsorption capacity C_e (mg/L): adsorbate concentration in equilibrium q_{max} (mg/g): Langmuir constant related to the maximum biosorption capacity b: Langmuir constant related to the affinity between sorbent and sorbate
Freundlich	$\ln q_e = \ln K_F + \frac{1}{n} \ln C_e$ $R_L = \frac{1}{1 + bC_o}$	K_F (L/g): constant equilibrium n: constant related to the affinity between sorbent and sorbate. b (L/mg): Langmuir constant C_o (mg/L): initial concentration of adsorbate R_L provides important information on the nature of the biosorption, 0 <R_L <1 denotes favorable adsorption, R_L> 1 indicates unfavorable adsorption

Source:(Tran *et al*., 2016).

The thermodynamic parameters of Gibbs free energy change (ΔG), enthalpy change (ΔH), and entropy change (ΔS) were estimated using the following equations:

$$\Delta G = -RT \ln K_c \tag{3}$$

$$\Delta G = \Delta H - T\Delta S \tag{4}$$

$$K_c = \frac{c_{es}}{c_e} \tag{5}$$

$$\ln K_c = \frac{\Delta S}{R} - \frac{\Delta H}{RT} \tag{6}$$

where: K_c is the equilibrium adsorption constant, C_{es} is the concentration of MB in the biosorbent at equilibrium, C_e is the concentration of MB in solution at equilibrium, R is the universal gas constant (8.314 J/mol.K) and T is the absolute temperature of the solution (K).

The desorption efficiency of the NC biomass was calculated using the following equation (Nayak & Pal, 2017):

$$\text{Desorption efficiency } \% = \frac{\text{amount of MB desorbed from NC}}{\text{amount of MB adsorbed on NC}} \times 100 \tag{7}$$

3 Results and discussion

3.1 *Characterization of biosorbent*

Figure 1 shows the FTIR spectrum of the NC biosorbent, the presence of broadband at 3427.3 cm^{-1} can be observed, it is indicated by the existence of -OH groups of polymeric compounds such as sucrose and the -NH group of proteins. The absorption band at 2931.6 cm^{-1} is due to the symmetric stretching of aliphatic chains of the typical C-H bond in alkyl functional groups of carbohydrate and its bending vibrations at 1388.7 cm^{-1} (Calero *et al*., 2013). Also, the absorption band at 1643.2 cm^{-1} can be seen due to the stretching of the bonds in the carbonyl groups (C=O) in primary and secondary amides of protein-peptide bonds (Gupta & Rastogi, 2008), and the band at 1546.8 cm^{-1} confirms the presence of carboxylates (COO- (Tran *et al*., 2016). According to Bhunia *et al*. (2018) the absorption bands at 1031.8 cm^{-1} and 1417.6 cm^{-1} are due to the stretching of the C-OH and C-H bond, respectively, in pyranose units. The FTIR spectrum of NC of the present study is similar to the FTIR spectrum of exopolysaccharides (EPS) reported by Ohki *et al*. (2014), who identify negatively charged groups such as carboxyl, hydroxyl, and amino to which the uptake of cationic molecules with MB can be attributed due to the electrostatic attraction between them. After MB had been adsorbed onto the NC surface, the spectrum showed several changes. As observed in Fig. 1, spectrum b, the band

at 3427.3 cm^{-1} shifted to 3498.3 cm^{-1} indicating that the functional groups such as O-H and N-H on the NC surface actively participated in the MB biosorption. In addition, the bands at 2931.6, 1643.2, 1546.8 y 1388.7 cm^{-1} shifted to 2993.2, 1710.4, 1630.8 y 1453.1 cm^{-1}, respectively. These changes are caused due to the adsorption of MB as well as due to the electrostatic interactions between MB and NC biosorbent (Nayak & Pal, 2017). The number of acid groups determined by the Boehm method was 0.52 mmolH^+/g, which shows that NC has acid surface, this may be due to the presence of functional groups reported in the analysis of the FTIR spectrum.

Figure 2 shows the characterization by Scanning Electron Spectroscopy (SEM), the morphology of the biosorbent surface (NC) is observed before and after biosorption; in Figure 2A a heterogeneous surface and the presence of cavities are observed, which would allow that MB molecules penetrate the NC and interact with it (Daneshvar *et al*., 2017).

On the other hand, after biosorption (Fig. 2A) a more homogeneous surface morphology is observed, with fewer cavities. This is due to the occupation of the biosorbent surface by the dye molecules (Albadarin & Mangwandi, 2015). This is corroborated with the intraparticle diffusion study shown below.

The p_{HPZC} is the pH at which the net surface charge in the biosorbent is zero, the p_{HPZC} value obtained was 1.5 (fig. 3). Therefore, in a solution with pH> p_{HPZC}, the surface is negatively charged and cation biosorption is favored due to the increasing electrostatic attraction between cationic dye molecules and NC functional groups (Lebron *et al*., 2018).

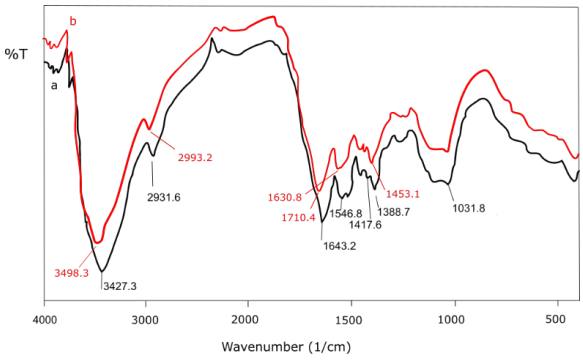

Fig. 1. Fourier Transform Infrared Spectroscopy (FTIR) spectrum of the biomass of the *Nostoc commune* (a) before and (b) after the MB adsorption.

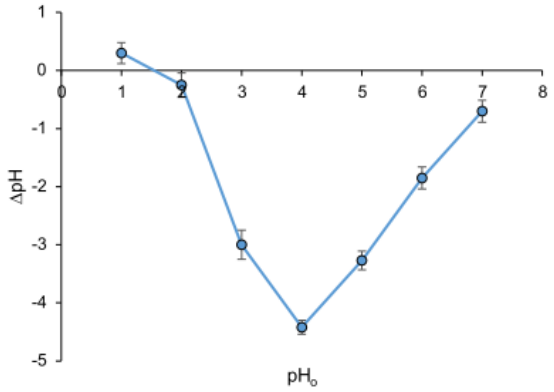

Fig. 3. Point zero charge (p_{HPZC}) of *Nostoc commune*.

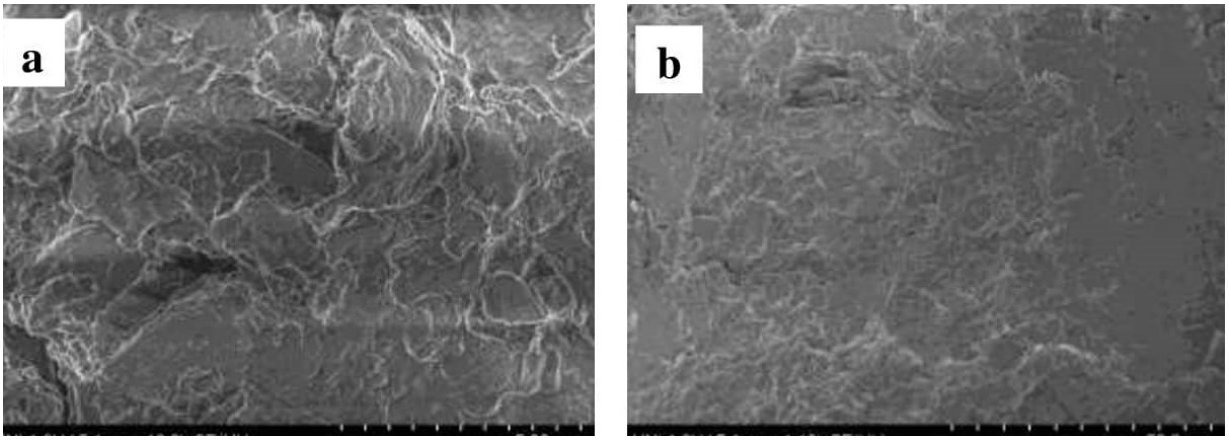

Fig. 2. Scanning electron microscope (SEM) of *Nostoc commune* (NC) a) Before biosorption and b) After biosorption.

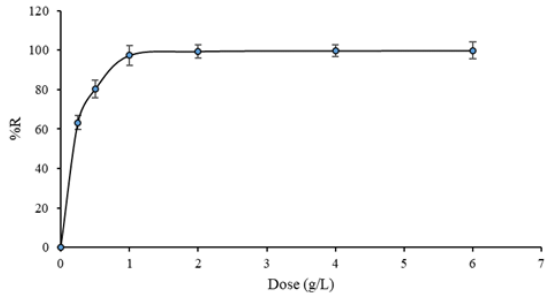

Fig. 4. Influence of the dose (NC) on the % Removal of MB, t = 60 min, T = 293 K, C_o = 50 mg/L.

3.2 Effect of biosorbent dose

Figure 4 shows the effect of the NC dose on the removal of MB that was studied in the range of 0.25 to 6 g/L, keeping the initial concentration of MB fixed at 50 mg/L, it is observed that the % elimination is increased from 66.3% to 99.78% with a dose increase from 0.25 to 6 g/L. This behavior could be attributed to the greater availability of active adsorption sites, due to the greater amount of NC biosorbent with a fixed volume of dye solution (Nayak & Pal, 2017), the highest removal percentage was achieved with the dose of biosorbent of 2 g/L, at higher concentrations the elimination of MB remained almost constant. Therefore, 1 g/L dose of NC was used as the optimal dose of biosorbent for the additional experiments. Similar behavior was reported by Afroze *et al*. (2015) and Albadarin *et al*. (2018) who removed the MB with the biomass of the eucalyptus bark and biomass of yerba mate respectively.

3.3 Effect of contact time and biosorption kinetics

In figure 5 it can be seen that, for the different initial concentrations, the biosorption capacity increased rapidly in the first 10 min and then increased slowly until reaching equilibrium at 60 min. The initial rapid phase can be attributed to the existence of a surface with unsaturated active sites. As the adsorption sites on the surface fill, the rate of biosorption decreases with additional contact time. Several investigators reported similar results regarding the equilibrium time for MB adsorption on dry bean powder (Shooto *et al*., 2020), algae (Moghazy *et al*., 2019), green and brown algae (Daneshvar *et al*., 2017).

With the experimental data, the kinetic parameters were calculated after plotting Log (q_e-qt) vs t (Figure 6a) and t/qt vs t (Figure 6b) and qt vs $t^{0.5}$ (Figure 6c) for the pseudo-first-order equation, pseudo-second-order and second linear section of the intraparticle diffusion equation, respectively. The results are presented in Table 3. It is observed that for all the initial concentrations of MB the data better fit the pseudo-second-order model (0.9992 $<R^2$ <0.9997). This suggests that the biosorption is controlled by chemisorption, which involves the exchange of electrons between the MB cations and the functional groups the surface of the NC (Mitrogiannis *et al*., 2015).

The intraparticle diffusion model was used to evaluate the contribution of MB diffusion within the NC biomass in the biosorption process (Figure 7c and 7d). It is observed that, for the three different initial concentrations, the behavior was not linear and the graph did not pass through the origin, which confirms that diffusion is not the only step that controls the rate of biosorption (Modesto *et al*., 2010). On the other hand, the intraparticle stage has a steeper slope at the higher MB concentration. "K_{id}" and "B" values increased as the initial dye concentration increased from 20 to 100 mg/L.

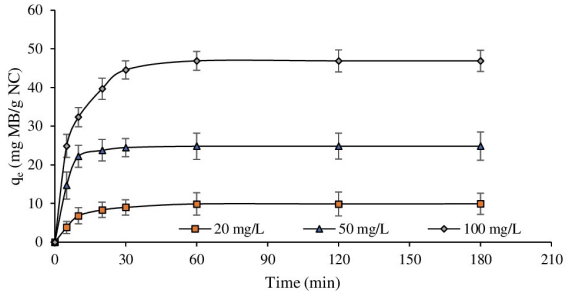

Fig. 5. Effect of contact time on methylene blue (MB) biosorption, *Nostoc commune* (NC) dose = 1g/L, T = 293 K.

Table 3. Kinetic parameters for MB biosorption on NC.

C_o	pseudo-first-order			Pseudo-second-order				intraparticular diffusion		
mg/L	k_1	$q_{e(cal)}$	R^2	$q_{e(cal)}$	h	k_2	R^2	K_{id}	B	R^2
20	0.004 ±0.001	44.52 ±2.8	0.8307	10.27±2.4	2.01 ±1.7	0.019 ±0.001	0.9992	0.944 ±0.05	3.92 ±0.92	0.9791
50	0.243 ±0.012	36.97 ±2.3	0.9436	24.75±1.8	20.04 ±2.1	0.032 ±0.013	0.9997	0.993 ±0.03	19.16 ±1.81	0.9831
100	0.013 ±0.001	70.76 ±1.9	0.9715	48.08±1.4	13.09 ±2.9	0.006 ±0.001	0.9996	3.012±0.04	21.61 ±2.11	0.6817

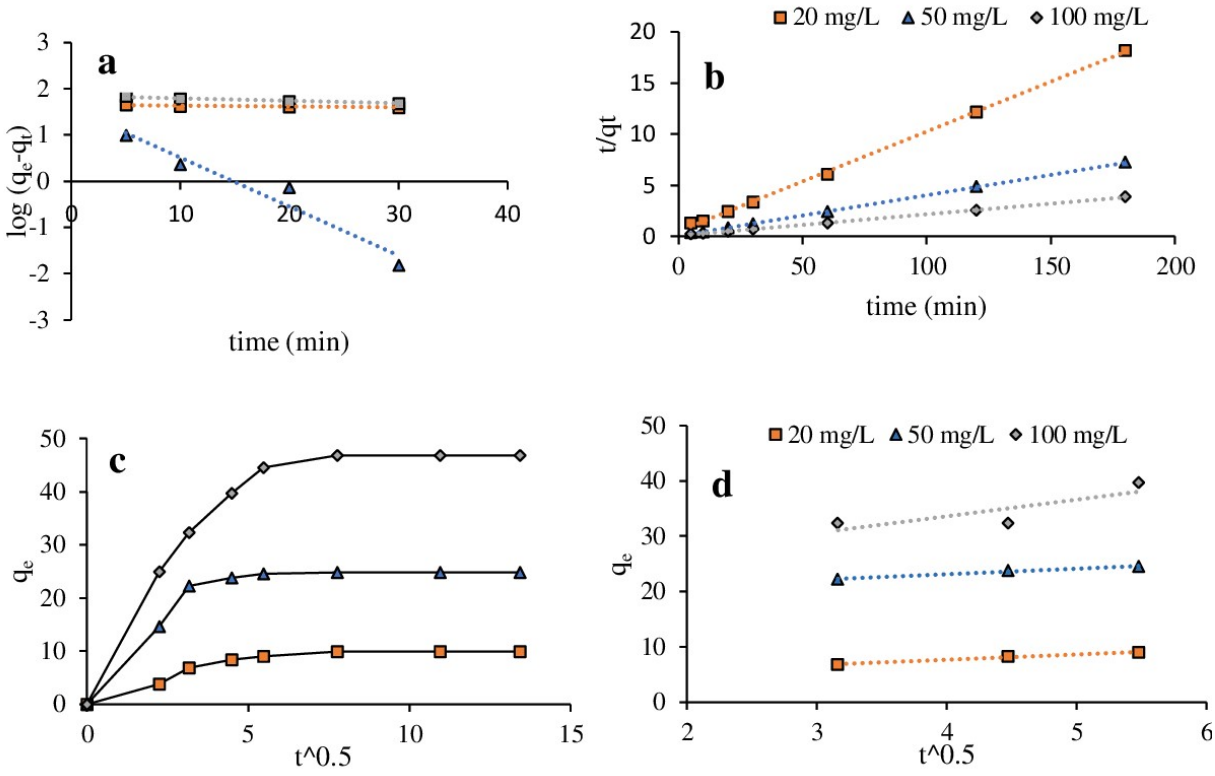

Fig. 6. MB biosorption kinetics on NC a) pseudo-first-order b) pseudo-second-order c) intraparticle diffusion d) second linear portion of the intraparticle diffusion model q_e Vs $t^{0.5}$.

This increase may be related to the increasing effect of the driving force that could reduce the diffusion of the colorant in the boundary layer and improve the diffusion in the solid (Daneshvar *et al*., 2017).

Figure 7 shows the effect of the initial MB concentration on the equilibrium biosorption capacity of NC at different pH values. It is observed that q_e increases with the increase in the initial concentration of MB at all pH values. For the lowest concentration of 20 mg/L and pH 8, the amount of MB removed was 9.9 mg/L and it increased to 90.67 mg/g with the highest initial concentration of MB of 200 mg/L. The same trend is observed for all pH values. This observation can be explained by the increasing driving force that overcomes the resistance to mass transfer of the MB dye between the aqueous and solid phase (Anastopoulos *et al*., 2017).

Furthermore, the number of collisions between the MB cations and the biosorbent may increase due to the increase in the initial concentration of dye, which would improve the sorption process (Mitrogiannis *et al*., 2015). The increasing driving force at higher dye concentrations is consistent with the values of the initial adsorption rate, h, (table 3) that were estimated by the parameters of the pseudo second order kinetic model. The influence of pH on q_e is also observed, this behavior is discussed and explained later.

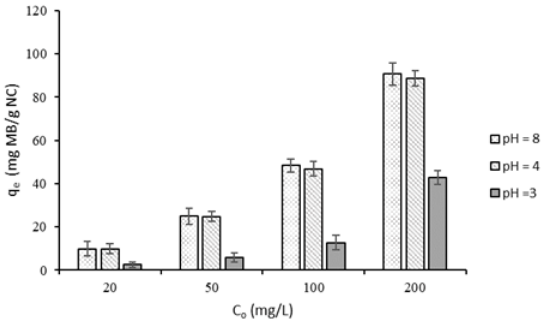

Fig. 7. Effect of initial MB concentration on NC adsorption capacity at different pH values, NC dose = 1g/L, t = 60 min, T = 293 K.

Table 4. Langmuir and Freundlich constants.

	Langmuir			**Freundlich**		
pH	q_{max}	**b**	R^2	**1/n**	K_F	R^2
3	103.09 ±5.4	0.049 ±0.012	0.991	0.746 ±0.02	4.22 ±0.98	0.9111
4	151.52 ±6.3	0.136 ±0.09	0.9811	0.470 ±0.01	22.21 ±3.25	0.9423
8	158.73 ±6.9	0.165 ±0.08	0.9814	0.286 ±0.01	38.84 ±4.12	0.9035

3.4 Adsorption isotherms

The biosorption isotherms show the relationship between the MB concentration in the liquid phase and the amount of MB adsorbed per unit weight of biosorbent at equilibrium Figure 8 shows the equilibrium isotherms for different pH values, the experimental data were analyzed using two common isotherm models: Langmuir and Freundlich.

The Langmuir constants (q_{max} and b) and Freundlich (K_F y n) were calculated from the slope and the intercept of the line graphs C_e/q_e versus C_e and log q_e versus log C_e respectively (Figure 9a and Figure 9b) and are presented in Table 4. The Langmuir and Freundlich isotherm models presented satisfactory and similar correlation coefficients (R^2> 0.98 and 0.90, respectively). The good and similar concordance of the two isotherm models applied with the experimental data shows that the sorption of MB was a complex process, involving more than one mechanism. Both the monolayer biosorption and the heterogeneity of the biosorbent surface affected the removal of MB from the solution (Mitrogiannis *et al*., 2015).

The values of the dimensionless separation factor, R_L, according to figure 10 are less than unity and greater than zero (0 <R_L <1) at all initial concentrations and pH, which confirms a favorable sorption process, the higher the Initial MB concentration, the lower the R_L value and the more favorable the MB biosorption (Albadarin & Mangwandi, 2015). On the other hand, the value of the values of 1/n were less than 1, which shows that the biosorption isotherm is classified as type L with high affinity between the dye molecules and the biosorbent (Ahmad *et al*., 2020; Deniz & Ersanli, 2019).

Table 4 shows that as the pH of the solution increases, the maximum adsorption capacity in monolayer also increases, as do the values of b, which shows a greater affinity of biomass for MB.

Compared with other studies of biosorption of MB reported in the literature (Table 5), the high values of q_{max} demonstrate that the material NC has great potential for use in eliminating the MB aqueous media.

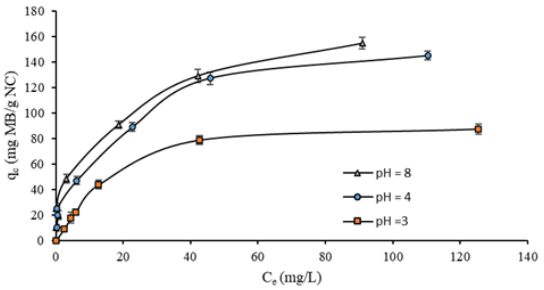

Fig. 8. Isotherms of the equilibrium of MB biosorption on NC, NC dose = 1g/L, t = 60 min, T = 293 K.

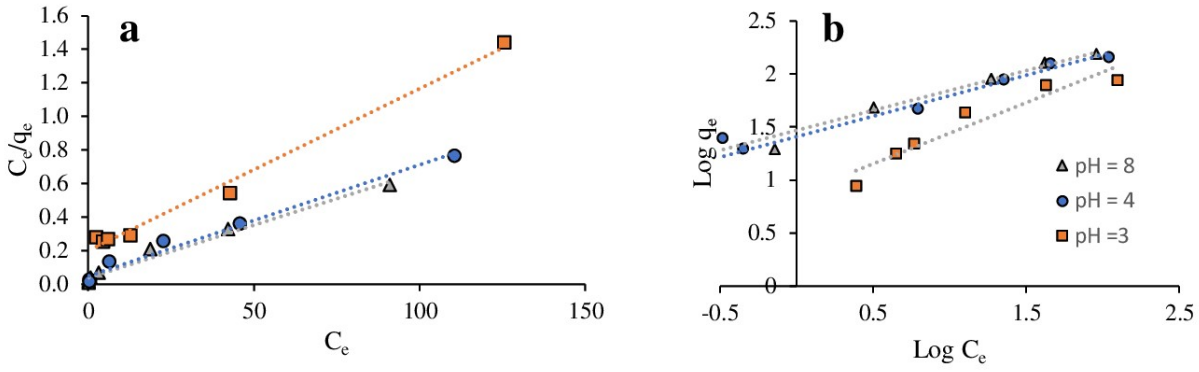

Fig. 9. Linear form of a) Langmuir equation b) Freundlich equation.

Table 5. Comparative table of the qe, of MB with different types of biomass.

Biosorbent material	q_{max} **(mg/g)**	**Reference**
Bibalvos powder	one	(Elwakeel *et al*., 2017)
Cumin seeds	13.62	(Shooto *et al*., 2020)
Gracilaria corticata algae	95.41	(Vijayaraghavan *et al*., 2015)
Seeds of *Abelmoschus esculentus*	104.38	(Nayak & Pal, 2017)
Green algae	143.97	(Daneshvar *et al*., 2017)
Cyanobacterium *Nostoc commune*	158.70	This studio

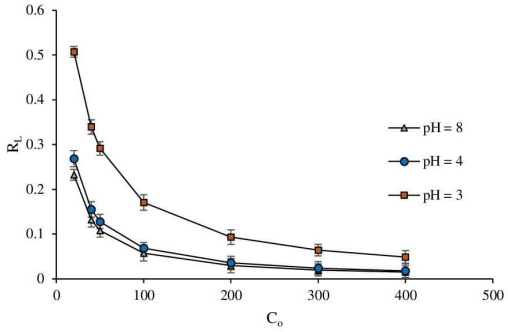

Fig. 10. Relationship between the initial concentration of MB and the dimensionless separation factor R_L at different pH values.

3.5 *Effect of pH*

The pH of the solution plays an important role in the biosorption process, as it affects both the chemistry of the solution and the binding sites to the surface of the biosorbent (Han *et al*., 2020). The initial pH of the MB solution was studied in a range from 1 to 8 (Fig. 11). For the three different initial concentrations, it is observed that the profiles have the same tendency, q_e increases with increasing pH. For NC the main functional groups are the hydroxyl and carboxyl, at pH acid the ionization of the carboxyl group would be low so that the electrostatic interaction between these functional groups and MB is weak; which is reflected in the low values of q_e.

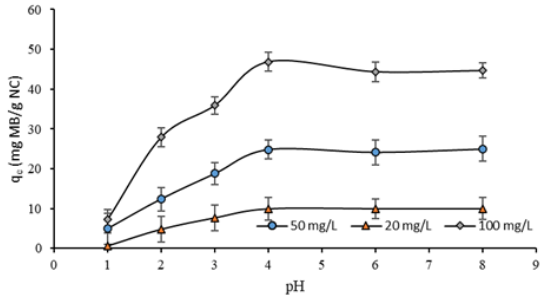

Fig. 11. Influence of pH on the ability of biosorption, NC dose = 1g/L, t = 60 min, T = 293K.

As the pH is increased, the sites of carboxylic acid are deprotonated and the carboxyl groups ionize into -COO-, whereby the capacity of biosorption of l MB increases (Yanqiao *et al*., 2014). On the other hand, the value of the point of zero charge (p_{HPZC}) of the NC is 1.5; when pH> p_{HPZC}, the surface of NC is negatively charged so could remove the cationic dye MB by electrostatic attraction evidenced with increasing capacity biosorption (Elwakeel *et al*., 2017).

3.6 *Thermodynamic study*

MB adsorption on NC was evaluated concerning thermodynamic parameters such as ΔG, ΔH, and ΔS calculated by equations (10) (11) (12) and (13). The ΔS and ΔH values were calculated from the intercept and slope of the $\ln K_c$ versus 1/T plot, respectively. As shown in Figure 12, the values of the correlation coefficient (R^2) were 0.98 and 0.96 for initial MB concentrations of 100 and 200 mg/L respectively, indicating that the estimated values of ΔH and ΔS are reliable. The calculated thermodynamic parameters are summarized in Table 6.

The negative ΔG values at the three temperatures evaluated represent the spontaneity and viability of the adsorption process with a high preference of the NC biosorbent for the MB dye (Nayak & Pal, 2017). It is observed that the negative value of ΔG is high at low temperature (298 K), which favors the adsorption process. On the other hand, the negative value of ΔH indicates that the adsorption process is exothermic (Alver *et al*., 2020). Therefore, the increase in temperature causes a decrease in the adsorption capacity of MB over NC.

The exothermic nature of the biosorption was also reported by other authors such as Dotto *et al*. (2013) and Cardoso *et al*. (2012) who removed synthetic dyes with a cyanobacterium (*Spirulina platensis*). According to Mitrogiannis *et al*. (2015) and Koyuncu & Kul, (2020), the magnitude of the enthalpy change can be used to classify the type of interaction between sorbent and sorbate.

Table 6. Thermodynamic parameters of MB biosorption on NC.

C_o		ΔS **kJ/mol**	ΔG **(kJ/mol)**		
mg/L	ΔH **kJ/mol**	**K**	**293 K**	**303 K**	**313 K**
100	- 34.13 ±3.25	-0.07 ±0.01	- 8.31 ±1.23	-7.20 ±1.56	-6.56 ±1.28
200	-41.14 ±4.12	-0.12 ±0.03	-5.54 ±1.56	-3.86 ±0.98	-3.12 ±0.82

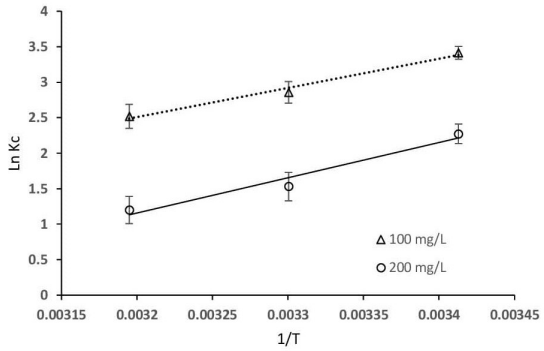

Fig. 12. $\ln K_c$ Vs a 1/T for the estimation of the thermodynamic parameters of the MB biosorption in NC.

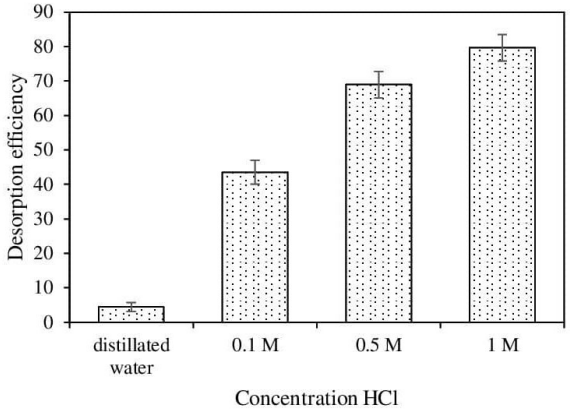

Fig. 13. Desorption of MB with different concentrations of HCl.

Values of ΔH <30 kJ/mol indicate physical sorption, values in the range of 4 to 10 kJ/mol show the existence of van der Waals forces. Values of 40 kJ/mol indicate ion exchange and values of 2 to 29 kJ/mol dipole bond forces. On the other hand, ΔH> 80 kJ/mol indicates chemical bonding forces. In this study, the values of ΔH (<42 kJ/mol) obtained would indicate that the biosorption of MB in the NC biomass is due to ion exchange. The negative effect of the increase in temperature on q_e and the good correlation of the pseudo-second-order kinetic model show that the sorption process of MB would involve chemisorption. Negative ΔS values for initial concentrations of 100 and 200 mg MB/L are very low, indicating that there are no notable changes in entropy and a decrease in disorder at the solid-liquid interface during MB biosorption in the NC (see Table 6).

3.7 Desorption studies

Desorption studies were carried out to evaluate the possibility of recovery of the dye, reuse of the biosorbent material, and a better understanding of the biosorption mechanism. Figure 13 shows the percentage of desorption of MB using distilled water and different concentrations of HCl (0.1, 0.5, and 1M). It is observed that the maximum desorption occurs using 1 M HCl, with an MB recovery of up to 81.64%.

This behavior would indicate that the mechanism of MB adsorption on the NC would be ion exchange (Anastopoulos *et al*., 2018). This result corroborates what was discussed in the thermodynamic study above. It is observed that the use of HCl for the desorption of MB allows the efficient regeneration of NC making it economically feasible (Eren *et al*., 2020).

Conclusions

The present study explores *Nostoc commune* powder (NC) as an efficient and effective biosorbent for removing methylene blue (MB), a cationic dye from aqueous media. With the analysis of the FTIR spectrum, it was possible to identify some representative functional groups of the polysaccharides which would be responsible for the removal of MB. FTIR analysis confirmed the interactions between NC biosorbent surface and MB dye molecule. The SEM analysis showed a heterogeneous surface and the presence of cavities in NC. Kinetic experiments clearly indicated that adsorption of MB dye on NC biomass is a multi-step process: a rapid adsorption of dye onto the

external surface followed by intra-particle diffusion into the interior of adsorbent which has also been confirmed by intra-particle diffusion model. The kinetic studies showed that the MB dye adsorption process followed pseudo-second-order kinetic model. The Langmuir isotherm better describes the experimental data at equilibrium, characterizing the process with the formation of a monolayer, the q_{max} was 158.7 mg/g. The good fit for the mentioned models and the results of the desorption study would indicate that the MB biosorption mechanism would occur through a chemisorption process specifically ionic exchange and would involve adsorption on the surface of the NC and intraparticle diffusion in the biomass pores. The amount of MB dye adsorption on NC was found to increase with an increase in initial solution pH and contact time. Thermodynamic parameters were determined at three different temperatures. From the results of negative enthalpy change (ΔH) accompanied by negative entropy change (ΔS) and negative decrease in Gibbs free energy change (ΔG), it is evident that the adsorption process is exothermic, favorable and spontaneous in nature. *Nostoc commune* can be used as an effective and environmentally friendly biosorbent for the removal of MB from wastewater

Acknowledgements

The authors thank the Continental University for financing this research work (Grant No: 064-2015/DI-UC), the Brazilian National Council for Scientific Development (CNPq, Grant Nº 407097/20), as well as Dr. Clemente Luyo of the National Engineering University for the facilities to perform the SEM analyzes.

References

Adhikari, B.K., Barrington, S., Martinez, J., King, S. (2009). Effectiveness of three bulking agents for food waste composting. *Waste Manage 29*, 197-203.

Afroze, S., Sen, T. K., Ang, M., & Nishioka, H. (2015). Adsorption of methylene blue dye from aqueous solution by novel biomass *Eucalyptus sheathiana* bark: equilibrium, kinetics, thermodynamics and mechanism. *Desalination and Water Treatment*, 1-21. https://doi.org/10.1080/19443994.2015.1004115

Ahmad, A., Khan, N., Giri, B. S., Chowdhary, P., & Chaturvedi, P. (2020). Removal of methylene blue dye using rice husk, cow dung and sludge biochar: Characterization, application, and kinetic studies. *Bioresource Technology 306*, 123202. https://doi.org/10.1016/j.biortech.2020.123202

Akbari, M., Hallajisani, A., Keshtkar, A. R., Shahbeig, H., & Ali Ghorbanian, S. (2015). Equilibrium and kinetic study and modeling of Cu(II) and Co(II) synergistic biosorption from Cu(II)-Co(II) single and binary mixtures on brown algae *C. indica. Journal of Environmental Chemical Engineering 3*, 140-149. https://doi.org/10.1016/j.jece.2014.11.004

Albadarin, A. B., & Mangwandi, C. (2015). Mechanisms of Alizarin red and methylene blue biosorption onto olive stone by-product: Isotherm study in single and binary systems. *Journal of Environmental Management 164*, 86-93. https://doi.org/10.1016/j.jenvman.2015.08.040

Albadarin, A. B., Solomon, S., Daher, M. A., & Walker, G. (2018). Efficient removal of anionic and cationic dyes from aqueous systems using spent Yerba Mate "*Ilex paraguariensis*". *Journal of the Taiwan Institute of Chemical Engineers 82*, 144-155. https://doi.org/10.1016/j.jtice.2017.11.012

Alver, E., Metin, A. Ü., & Brouers, F. (2020). Methylene blue adsorption on magnetic alginate/rice husk bio-composite. *International Journal of Biological Macromolecules 154*, 104-113. https://doi.org/10.1016/j.ijbiomac.2020.02.330

Anastopoulos, I., Karamesouti, M., Mitropoulos, A. C., & Kyzas, G. Z. (2017). A review for coffee adsorbents. *Journal of Molecular Liquids 229*, 555-565. https://doi.org/10.1016/j.molliq.2016.12.096

Anastopoulos, I., Margiotoudis, I., & Massas, I. (2018). The use of olive tree pruning waste compost to sequestrate methylene blue dye from aqueous solution. *International Journal of*

Phytoremediation 20, 831-838. https://doi.org/10.1080/15226514.2018.1438353

Aygun, A., Yenisoy-Karakas, S., Duman, I. (2003). Production of granular activated carbon from fruit stones and nutshells and evaluation of their physical, chemical and adsorption properties. *Microporous and Mesoporous Materials 66*, 189-195. https://doi.org/10.1016/j.micromeso.2003.08.028

Bhunia, B., Shankar, U., Uday, P., Oinam, G., & Mondal, A. (2018). Characterization, genetic regulation and production of cyanobacterial exopolysaccharides and its applicability for heavy metal removal. *Carbohydrate Polymers 179*, 228-243. https://doi.org/10.1016/j.carbpol.2017.09.091

Calero, M., Pérez, A., Blázquez, G., Ronda, A., & Martín-lara, M. A. (2013). Characterization of chemically modified biosorbents from olive tree pruning for the biosorption of lead. *Ecological Engineering 58*, 344-354. https://doi.org/10.1016/j.ecoleng.2013.07.012

Cardoso, N. F., Lima, E. C., Royer, B., Bach, M. V., Dotto, G. L., Pinto, L. A. A., & Calvete, T. (2012). Comparison of *Spirulina platensis* microalgae and commercial activated carbon as adsorbents for the removal of Reactive Red 120 dye from aqueous effluents. *Journal of Hazardous Materials 241-242*, 146-153. https://doi.org/10.1016/j.jhazmat.2012.09.026

Daneshvar, E., Vazirzadeh, A., Niazi, A., Sillanpää, M., & Bhatnagar, A. (2017). A comparative study of methylene blue biosorption using different modified brown, red and green macroalgae - Effect of pretreatment. *Chemical Engineering Journal 307*, 435-446. https://doi.org/10.1016/j.cej.2016.08.093

Deniz, F., & Ersanli, E. T. (2019). A low-cost and eco-friendly biosorbent material for effective synthetic dye removal from aquatic environment: characterization, optimization, kinetic, isotherm and thermodynamic studies. *International Journal of Phytoremediation 0*, 1-10. https://doi.org/10.1080/15226514.2019.1663485

Diengdoh, O. L., & Syiem, M. B. (2017). Zn^{2+} sequestration by *Nostoc muscorum*: study of thermodynamics, equilibrium isotherms, and biosorption parameters for the metal. *Environmental Monitoring and Assessment 189*, 2-13. https://doi.org/10.1007/s10661-017-6013-4

Dotto, G. L., Vieira, M. L. G., Esquerdo, V. M., & Pinto, L. A. A. (2013). Equilibrium and thermodynamics of azo dyes biosorption onto *Spirulina platensis*. *Brazilian Journal of Chemical Engineering 30*, 13-21. https://doi.org/10.1590/S0104-66322013000100003

Elwakeel, K. Z., Elgarahy, A. M., & Mohammad, S. H. (2017). Journal of Environmental Chemical Engineering Use of beach bivalve shells located at Port Said coast (Egypt) as a green approach for methylene blue removal. *Biochemical Pharmacology 5*, 578-587. https://doi.org/10.1016/j.jece.2016.12.032

Eren, M., Arslanoğlu, H., & Çiftçi, H. (2020). Production of microporous Cu-doped BTC (Cu-BTC) metal-organic framework composite materials, superior adsorbents for the removal of methylene blue (Basic Blue 9). *Journal of Environmental Chemical Engineering 8*, 104247. https://doi.org/10.1016/j.jece.2020.104247

Fomina, M., & Gadd, G. M. (2014). Biosorption: Current perspectives on concept, definition and application. *Bioresource Technology 160*, 3-14. https://doi.org/10.1016/j.biortech.2013.12.102

Gupta, V. K., & Rastogi, A. (2008). Biosorption of lead (II) from aqueous solutions by non-living algal biomass *Oedogonium* sp . and *Nostoc* sp.−A comparative study. *Colloids and Surfaces B: Biointerfaces 64*, 170-178. https://doi.org/10.1016/j.colsurfb.2008.01.019

Han, Q., Wang, J., Goodman, B. A., Xie, J., & Liu, Z. (2020). High adsorption of methylene blue by activated carbon prepared from phosphoric acid treated eucalyptus residue. *Powder Technology 366*, 239-248. https://doi.org/10.1016/j.powtec.2020.02.013

Koyuncu, H., & Kul, A. R. (2020). Biosorption study for removal of methylene blue dye from aqueous solution using a novel activated carbon

obtained from nonliving lichen (*Pseudevernia furfuracea* (L.) Zopf.). *Surfaces and Interfaces 19*, 100527. https://doi.org/10.1016/j.surfin.2020.100527

Lebron, Y. A. R., Moreira, V. R., Santos, L. V. S., & Jacob, R. S. (2018). Remediation of methylene blue from aqueous solution by *Chlorella pyrenoidosa* and *Spirulina maxima* biosorption: Equilibrium, kinetics, thermodynamics and optimization studies. *Journal of Environmental Chemical Engineering 6*, 6680-6690. https://doi.org/10.1016/j.jece.2018.10.025

Mitrogiannis, D., Markou, G., Çelekli, A., & Bozkurt, H. (2015). Biosorption of methylene blue onto Arthrospira platensis biomass: Kinetic, equilibrium and thermodynamic studies. *Journal of Environmental Chemical Engineering 3*, 670-680. https://doi.org/10.1016/j.jece.2015.02.008

Modesto, S., Brito, D. O., Martins, H., Andrade, C., Frota, L., Pires, R., & Azevedo, D. (2010). Brazil nut shells as a new biosorbent to remove methylene blue and indigo carmine from aqueous solutions. *Journal of Hazardous Materials 174*, 84-92. https://doi.org/10.1016/j.jhazmat.2009.09.020

Moghazy, R. M., Labena, A., & Husien, S. (2019). Eco-friendly complementary biosorption process of methylene blue using micro-sized dried biosorbents of two macro-algal species (*Ulva fasciata* and *Sargassum dentifolium*): Full factorial design, equilibrium and Kinetic studies. *International Journal of Biological Macromolecules 134*, 330-343. https://doi.org/10.1016/j.ijbiomac.2019.04.207

Morsy, F. M., Hassan, S. H. A., Koutb, M., National, K., Science, A., & Arabia, S. (2011). Biosorption of Cd (II) and Zn (II) by *Nostoc commune*: Isotherm and Kinetics Studies. *Clean - Soil, Air, Water 39*, 680-687. https://doi.org/10.1002/clen.201000312

Nayak, A. K., & Pal, A. (2017). Green and ef fi cient biosorptive removal of methylene blue by *Abelmoschus esculentus* seed: Process optimization and multi-variate modeling. *Journal of Environmental Management 200*, 145-159. https://doi.org/10.1016/j.jenvman.2017.05.045

Ohki, K., Le, N. Q. T., Yoshikawa, S., Kanesaki, Y., Okajima, M., Kaneko, T., & Thi, T. H. (2014). Exopolysaccharide production by a unicellular freshwater cyanobacterium *Cyanothece* sp. isolated from a rice field in Vietnam. *Journal of Applied Phycology 26*, 265-272. https://doi.org/10.1007/s10811-013-0094-4

Patel, A., Matsakas, L., Rova, U., & Christakopoulos, P. (2019). Bioresource Technology A perspective on biotechnological applications of thermophilic microalgae and cyanobacteria. *Bioresource Technology 278(January)*, 424-434. https://doi.org/10.1016/j.biortech.2019.01.063

Salazar-Pinto, B. M., Zea-Linares, V., Villanueva-Salas, J. A., & Gonzales-Condori, E. G. (2021). Cd (II) and Pb (II) biosorption in aqueous solutions using agricultural residues of *Phaseolus vulgaris* L.: Optimization, kinetics, isotherms and desorption. *Revista Mexicana de Ingeniería Química 20*, 305-322. https://doi.org/10.24275/rmiq/IA1864

Shooto, N. D., Thabede, P. M., Bhila, B., Moloto, H., & Naidoo, E. B. (2020). Lead ions and methylene blue dye removal from aqueous solution by mucuna beans (velvet beans) adsorbents. *Journal of Environmental Chemical Engineering 8*, 103557. https://doi.org/10.1016/j.jece.2019.103557

Tatjana, D. Š., Petrovi, M. S., Pastor, F. T., Lon, D. R., Petrovi, J. T., Milojkovi, J. V, & Stojanovi, M. D. (2018). Study of heavy metals biosorption on native and alkali-treated apricot shells and its application in wastewater treatment. *Journal of Molecular Liquids 259*, 340-349. https://doi.org/10.1016/j.molliq.2018.03.055

Tejada-Tovar, C., Bonilla-Mancilla, H., del Pino-Moreyra, J., Villabona-Ortíz1, A., & Ortega-Toro, R. (2020). Efecto de la dosis de adsorbente en la remoción de Pb(II) usando bagazo de caña de azúcar: Cinética e isotermas. *Revista Mexicana de Ingeniería Química 19*, 1413-1423. http://rmiq.org/ojs311/index.php/rmiq/article/view/1101

Tran, H. T., Vu, N. D., Matsukawa, M., Okajima, M., Kaneko, T., Ohki, K., & Yoshikawa, S. (2016). Heavy metal biosorption from aqueous solutions by algae inhabiting rice paddies in

Vietnam. *Journal of Environmental Chemical Engineering 4*, 2529-2535. https://doi.org/10.1016/j.jece.2016.04.038

Wahlström, N., Steinhagen, S., Toth, G., Pavia, H., & Edlund, U. (2020). Ulvan dialdehyde-gelatin hydrogels for removal of heavy metals and methylene blue from aqueous solution. *Carbohydrate Polymers 249*, 116841. https://doi.org/10.1016/j.carbpol.2020.116841

Yagub, M. T., Sen, T. K., Afroze, S., & Ang, H. M. (2014). Dye and its removal from aqueous solution by adsorption: A review. *Advances in Colloid and Interface Science 209*, 172-184. https://doi.org/10.1016/j.cis.2014.04.002

Yanqiao, J. I. N., Yizhuan, Z., Qiufeng, L., & Xiansu, C. (2014). Biosorption of methylene blue by chemically modified cellulose waste. *Journal of Wuhan Technology-Mater*. University of Sci. Ed., 817-823. https://doi.org/10.1007/s11595-014-1003-7